Pergamon

Acta mater. Vol. 46, No. 13, pp. 4725–4732, 1998
© 1998 Acta Metallurgica Inc.
Published by Elsevier Science Ltd. All rights reserved
Printed in Great Britain
PII: S1359-6454(98)00122-0
1359-6454/98 $19.00 + 0.00

VISCOSITY OF THE SUPERCOOLED LIQUID AND RELAXATION AT THE GLASS TRANSITION OF THE $Zr_{46.75}Ti_{8.25}Cu_{7.5}Ni_{10}Be_{27.5}$ BULK METALLIC GLASS FORMING ALLOY

R. BUSCH†, E. BAKKE and W. L. JOHNSON

California Institute of Technology, W. M. Keck Laboratory of Engineering Materials, 138-78, Pasadena, CA 91125, U.S.A.

(Received 25 January 1998; accepted 28 March 1998)

Abstract—The flow and relaxation of the $Zr_{46.75}Ti_{8.25}Cu_{7.5}Ni_{10}Be_{27.5}$ bulk metallic glass forming alloy was investigated in the supercooled liquid state and the glass transition region using parallel plate rheometry, three-point beam bending as well as differential scanning calorimetry. The results indicate that this bulk metallic glass former is a strong liquid that, kinetically, behaves in a similar way as a silicate melt. The relaxation of the viscosity and specific heat capacity was investigated in isothermal experiments and with constant heating rates. The studies reveal that the relaxation of the viscosity into its equilibrium state is directly related to the calorimetric glass transition. The observed calorimetric glass transition in this strong glass former is of a purely kinetic nature and a thermodynamically metastable amorphous state cannot be observed in this bulk metallic glass forming liquid on a laboratory time scale. The heating rate dependence of the calorimetric glass transition reflects the fragility of the liquid. © *1998 Acta Metallurgica Inc. Published by Elsevier Science Ltd. All rights reserved.*

1. INTRODUCTION

After their discovery in 1960 by Duwez and co-workers [1], metallic glass forming liquids have been studied by a variety of methods with respect to their thermodynamic, kinetic and structural properties. Viscosity is the key parameter to describe the kinetic slowdown when a melt is undercooled below its liquidus temperature. The increase of viscosity with undercooling reflects the increasingly longer time scale for structural rearrangements in the supercooled liquid state. If the viscosity reaches a value of $\sim 10^{12}$ Pa s upon undercooling, the intrinsic time scale for maintaining metastable equilibrium becomes comparable to the laboratory time scales, i.e. the cooling time. The liquid freezes to a glass, namely it vitrifies.

In metallic systems glass formation could be observed up to recently only after rapidly quenching the melt with rates of the order of 10^4–10^6 K/s [2]. This resulted in thin ribbons or sheets with thicknesses of typically 20–50 μm. These metallic glasses showed a poor thermal stability with respect to crystallization in their undercooled (supercooled) liquid state when cooled below the melting point as well as when heated above their glass transition from the frozen-in glassy state into the metastable supercooled liquid state. Thus thermophysical properties could only be measured in small temperature ranges and large extrapolations had to be made to obtain the temperature dependence of the viscosity. Viscosities of metallic supercooled liquids close to the glass transition have been previously measured for example by Chen and Turnbull [3], Tsao and Spaepen [4] and others [5, 6]. The viscosities were determined in the glass transition region and crystallization did not allow measurements of the equilibrium viscosity below 10^9 Pa s or for long times to eliminate relaxation effects.

In recent years multicomponent alloy systems have been found that are much more robust with respect to crystallization and form bulk metallic glass. Examples are the La–Al–Ni [7], the Zr–Al–Ni–Cu [8] and the Zr–Ti–Cu–Ni–Be [9] alloy systems of which the latter one is by far the best bulk metallic glass former with critical cooling rates as low as 1 K/s [10]. Amorphous ingots typically up to 50 mm in the smallest dimension can be produced.

The high resistance with respect to crystallization allows for measurements of the thermophysical properties of these undercooled metallic liquids in a broad time and temperature range. For example, results have been obtained for the specific heat capacity [11], diffusion coefficients [12] or emissivity [13].

In this study viscosity measurements performed on these metallic glasses using parallel plate rheometry and three-point beam bending are presented. Both methods require bulk samples that were not available in the past. The viscosities are measured

†To whom all correspondence should be addressed.

in a large time and temperature range and compared with differential scanning calorimetry (DSC) measurements at the glass transition.

2. EXPERIMENTAL METHODS

Amorphous $Zr_{46.75}Ti_{8.25}Cu_{7.5}Ni_{10}Be_{27.5}$ alloys were prepared from the mixture of the elements of purity ranging from 99.5 to 99.9% by induction melting and subsequent water quenching in 6.35 and 10 mm inner diameter silica tubes. Cylindrical samples were cut from the 6.35 mm rods for use in parallel plate rheometry experiments. Beams of rectangular cross section were cut from the 10 mm rods for beam bending. The experimental apparatus used for both experiments was a Perkin-Elmer Thermal Mechanical Analyser (TMA 7).

Parallel plate rheometry as described by Stephan [14] and Diennes and Klemm [15] was used to study the viscosity of $Zr_{46.75}Ti_{8.25}Cu_{7.5}Ni_{10}Be_{27.5}$ between 10^9 and 10^5 Pa s as a function of temperature. A disc of the material flows in between two 3.7 mm diameter quartz penetration probes that were used as parallel plates. Measurements were performed with different heating rates and also isothermally using samples of different initial height. In the experiments the samples have to completely fill the area between the plates. In order to meet this condition the samples were first heated above the glass transition to 683 K where the material is fluid enough to fill the volume between the plates completely using small forces. Then the sample was cooled to 473 K and the viscosity measurement was started with the alloy firmly seated between the plates.

By measuring the height of the sample vs time, the viscosity at any temperature is given by the Stephan equation

$$\eta = -\frac{2Fh^3}{3\pi a^4 \frac{dh}{dt}} \tag{1}$$

where F is the applied load, a the radius of the plates, and h the height of the sample. Since equation (1) was derived by neglecting the velocity normal to the plates, the measured value of the viscosity [i.e. the value calculated according to equation (1)] depends on the aspect ratio between the sample height and the radius of the sample. The equilibrium viscosity can be determined by measuring the viscosity for different aspect ratios $x = h/a$ between height, h, and radius, a, of the plates and fitting the data with the parabolic function

$$\eta = b + cx^2. \tag{2}$$

The value of this function that corresponds to an aspect ratio of zero is the true viscosity (see also Refs [16, 17]).

Three-point beam bending is the other method that was applied to measure viscosity. With this technique viscosities in the range from 10^7 to 10^{14} Pa s can be measured. A beam that is supported at the ends by sharp edges is deflected with a constant force applied to the center of the beam. From the deflection rate the viscosity is determined by the equation [18–20]

$$\eta = -\frac{gL^3}{2.4 I_c v}\left(M + \frac{\rho AL}{1.6}\right) \tag{3}$$

where g is the gravitational constant (m/s^2), I_c the cross-section moment of inertia (m^4),† v the midpoint deflection rate (m/s), M the applied load (kg), ρ the density of the glass (kg/m^3), A the cross-sectional area (m^2), and L the support span (5.08×10^{-3} m for the apparatus). In the case of three-point beam bending the measured apparent viscosity is independent of the geometry of the beam. Beams with square and rectangular cross sections were used and gave consistent results.

Calorimetric measurements at the glass transition were performed in a Perkin Elmer DSC7 using different heating rates and isothermal experiments. The temperature scale of the DSC and the TMA were calibrated for each heating rate using the melting points of indium and zinc.

3. RESULTS

The viscosity measurements were performed either with constant heating rate or in isothermal experiments. Figure 1 shows a viscosity measurement by parallel plate rheometry performed at a heating rate of 0.833 K/s and a force of 2.6 N. The viscosity decreases with increasing temperature. At 743 K and a viscosity of 6.0×10^5 Pa s the material starts to crystallize resulting in a rising apparent viscosity. Below about 680 K the sample is subject

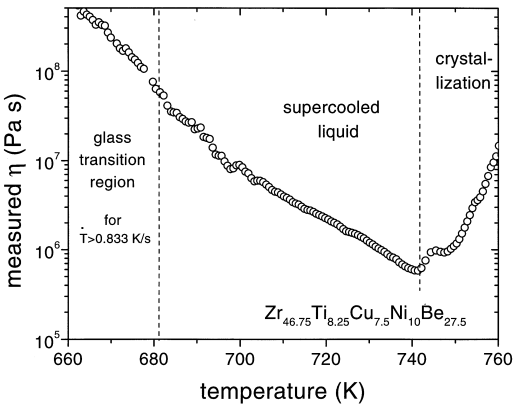

Fig. 1. Measured viscosity in the supercooled liquid for a heating rate of 0.833 K/s using parallel plate rheometry.

†The cross-section moment of inertia for a rectangular beam is $(a \cdot h^3)/3$, with, a, width and, h, height.

to relaxation processes due to the glass transition. In order to measure equilibrium viscosities in this range lower heating rates or isothermal measurements have to be conducted. Figure 2 summarizes the apparent viscosities measured by parallel plate rheometry at a temperature of 703 K. The flow between the plates was measured with different heating rates, isothermally and at different aspect ratios. The data were fitted with the parabolic equation (2) yielding an equilibrium value of 4.1×10^6 Pa s. Equilibrium viscosity data were obtained by parallel plate rheometry in a viscosity range between 10^5 and 10^9 Pa s (see Fig. 3). Viscosities in this range have not been measured in metallic supercooled liquids previously.

In order to measure higher viscosities in the glass transition region the three-point beam bending method was applied. In Fig. 3 beam bending data measured with a constant heating rate of 0.833 K/s (◇) and viscosity values, after equilibrating the material in isothermal beam bending experiments (●), are depicted. Furthermore, the equilibrium viscosity data obtained by parallel plate rheometry (○) are included.

The viscosity is compared with the calorimetric glass transition that is studied in a DSC with the same respective heating rate as the viscosity measurement. A DSC scan is included in Fig. 3. Three different regions can be distinguished. For the heating rate of 0.833 K/min the material is amorphous below 623 K. Between 623 and 673 K it undergoes the calorimetric glass transition indicated by the gradual increase of the specific heat capacity (endothermic heat flow) in the DSC scan. Above 650 K an overshooting is observed due to an enthalpy relaxation that is caused by the thermal history of the sample [21]. Beyond 673 K the material is a supercooled liquid.

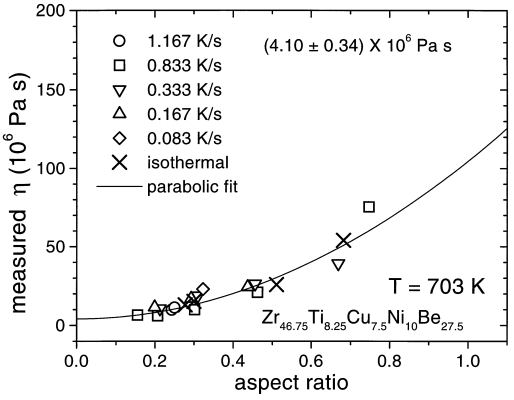

Fig. 2. Measured viscosity at a temperature of 703 K as a function of aspect ratio. Different heating rates and isothermal experiments are used. The data are fitted to a parabolic function. For all heating rates the material is above the glass transition and thus in metastable equilibrium.

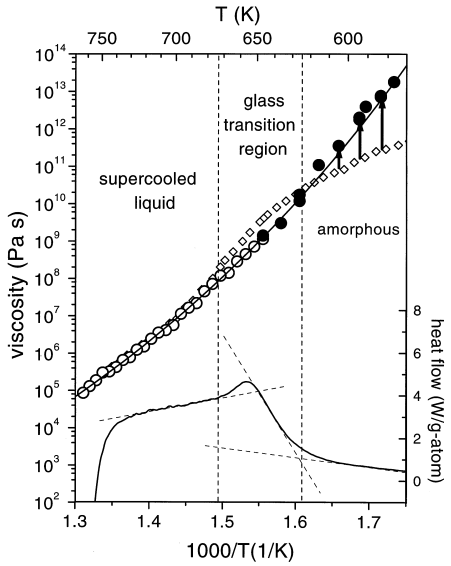

Fig. 3. Viscosity in the glass transition region, measured by beam bending with a constant heating rate of 0.833 K/s (◇) and viscosity values after equilibrating the material in isothermal beam bending experiments (●). The pathways of equilibration (indicated by arrows) are shown in Fig. 4. The equilibrium viscosity data obtained by parallel plate rheometry (○) and the equilibrium data by beam bending are in good agreement and are fitted well with a Vogel–Fulcher–Tammann relation. The fit is included in the figure. Also included is the DSC scan throughout the glass transition measured with 0.833 K/s. The calorimetric glass transition region agrees with the temperature and time window in which the viscosity reaches its equilibrium value.

The measured viscosity upon heating with constant rate undergoes the transition from the amorphous state to the supercooled liquid state in the same temperature range where the calorimetric glass transition is observed. Below 623 K the viscosity stays smaller than the equilibrium viscosity because of frozen-in free volume in the amorphous state. Above 673 K the measured viscosity corresponds to the equilibrium viscosity.

In general there is not one well-determined calorimetric glass transition temperature but a temperature interval in which the glass transition occurs. The location of this interval on the temperature axis depends on the heating or cooling rate. The calorimetric glass transition was measured in the DSC with different heating rates in the range between 8.33×10^{-3} and 5 K/s. The shift of the glass transition region with heating rate is shown in Fig. 4. For each heating rate three temperatures are drawn, the onset (○), the point of the steepest ascent (△), and the temperature where the supercooled liquid is reached (□) (see also Fig. 3). With increasing heating rate the glass transition is shifted to higher temperatures, because a shorter intrinsic relaxation time of the material is needed to reach the metastable equilibrium state of the supercooled liquid. In Fig. 4 the temperatures are included

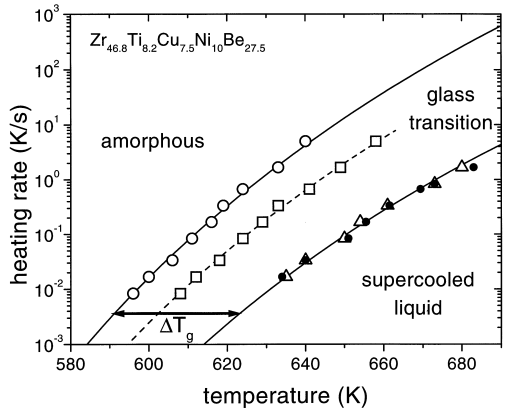

Fig. 4. Temperature range in which the glass transition region occurs as a function of heating rate measured in a DSC experiment. (○) marks the onset of the glass transition, (□) the temperature of the steepest ascent and (△) the temperature where the supercooled liquid is reached calorimetrically. The solid symbols (●) represent the temperatures at which the equilibrium viscosity is reached in measurements with constant heating rate. The data are fitted with a VFT-type equation.

where the measured viscosity reached the equilibrium value for each of the used heating rates (●). These temperatures are in good agreement with the values obtained from the DSC scans, where the specific heat capacity of the supercooled liquid is reached.

In order to measure the equilibrium viscosity for lower temperatures smaller heating rates or isothermal measurements have to be used. In the case of the beam bending experiments the samples were heated to a certain temperature at a rate of 0.833 K/s and the isothermal change of viscosity was monitored. In Fig. 5 three examples for the isothermal relaxation from the amorphous state into the supercooled liquid state are shown. The relaxation pathways are indicated in Fig. 3 by arrows. The relaxation processes in the glass transition region are usually not found to follow an exponential law but obey a stretched exponential function [22]. The viscosity relaxation was fitted with a stretched exponential relaxation function

$$\eta(t) = \eta_a + \eta_{eq\text{-}a} \cdot (1 - e^{-(t/\tau_s)^{\beta}}) \qquad (4)$$

in which, τ_s, is an average shear flow relaxation time, β, a stretching exponent, t, the time and, η_a, the viscosity of the amorphous alloy before relaxation. $\eta_{eq\text{-}a}$ is the total viscosity change during relaxation from the amorphous state into the equilibrium state. The fitted equilibrium viscosities [(●) in Fig. 3] reach values that are in good agreement with the extrapolation of the viscosities measured at higher temperatures by parallel plate rheometry.

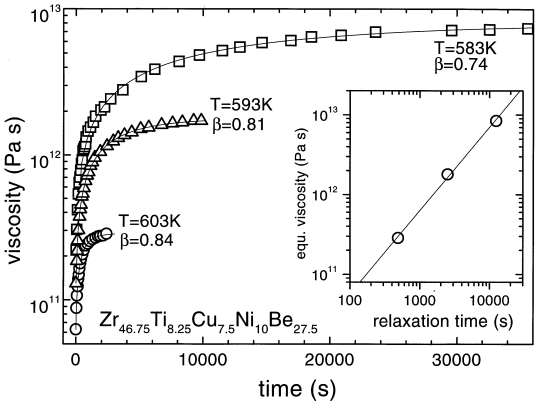

Fig. 5. Isothermal measurements of the viscosity using three-point beam bending. The data are fitted with a stretched exponential relaxation function. The inset shows the equilibrium viscosity as a function of relaxation time.

4. DISCUSSION

The measured equilibrium viscosities will be discussed in the framework of the fragility concept and compared with other metallic and non-metallic glass formers. It will be shown that temperature dependence of the equilibrium viscosity and the relaxation of the viscosity throughout the glass transition are consistent with the strong glassy nature of this bulk metallic glass. Since viscosity relaxation and the calorimetric glass transition occur on the same time scale, it will thus further be shown that the heating rate dependence of the calorimetric glass transition is a measure of the fragility of the material.

4.1. Strong liquid behavior

All equilibrium viscosity data obtained in the supercooled liquid can be described well with the Vogel–Fulcher–Tammann (VFT) relation

$$\eta = \eta_0 \cdot \exp[D^* \cdot T_0/(T - T_0)]. \qquad (5)$$

Equation (5) represents a formulation of the VFT relation that includes the fragility parameter, D^* [23], and the VFT temperature, T_0, where the barriers with respect to flow would go to infinity. In the best fit to the experimental data $T_0 = 372$ K and $D^* = 22.7$ are found. The fit is included in Fig. 3. The value η_0 was set as 4×10^{-5} Pa s according to the relation $\eta_0 = N_A \cdot h/V$, with, N_A, Avogadro's constant, h, Planck's constant and, V, the molar volume [24]. Masuhr [25, 26] measured high temperature viscosity above the melting point using capillary flow. This value is included in the fit (see also Fig. 6).

It is worthwhile mentioning that the observed VFT temperature for this metallic glass is much lower than the observed glass transition in the DSC, which is found at about 600 K on laboratory time scales [$(T_0 \approx 2/3 \cdot T_g)$, see Fig. 4]. T_0 is also much lower than the Kauzmann temperature $T_K = 560$ K [21] for this alloy. If the kinetic slowdown is entirely caused by the change of configurational entropy in the supercooled liquid, as it is

Edited by Foxit Reader
Copyright(C) by Foxit Software Company,2005-2008
For Evaluation Only.

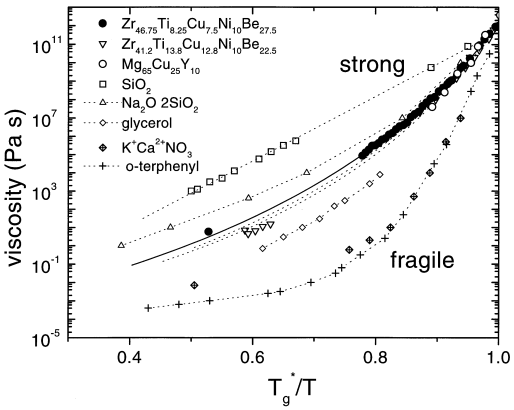

Fig. 6. Fragility plot of the viscosities of the $Zr_{46.75}Ti_{8.25}Cu_{7.5}Ni_{10}Be_{27.5}$ alloy, two other bulk metallic glasses [26, 28] and several non-metallic "strong" and "fragile" glasses. The data on non-metallic glasses were taken from Ref. [23].

assumed in the Adams–Gibbs model [27], the configurational entropy of the liquid would not vanish at the Kauzmann temperature but at a lower temperature close to the VFT temperature. In this picture, the supercooled liquid can, in principle, exist below the Kauzmann temperature and its entropy can become smaller than that of the crystalline mixture. This was also observed for the $Zr_{41.2}Ti_{13.8}Cu_{12.5}Ni_{10}Be_{22.5}$ [26] and the $Mg_{65}Cu_{25}Y_{10}$ [28] bulk metallic glass formers and may be characteristic for multicomponent glass forming alloys due to a large entropy of mixing in the crystalline state.

In Fig. 6 the experimental viscosity data for the bulk metallic glass forming liquid are compared with other glass forming liquids in the framework of the fragility concept (see, e.g. Ref. [23]). On this "Angell plot" the viscosity data for each material are normalized to the temperature, T_g^*, where the viscosity is found to be 10^{12} Pa s. The temperature dependence of the viscosity in open network glasses like SiO_2 can be described well by an Arrhenius law. These glass formers are called strong liquids and exhibit high equilibrium melt viscosities of the order of some 10^4 Pa s. The VFT temperature of strong liquids is far below the glass transition that is observed on a laboratory time scale. The other extremes are fragile glass formers like ionically bonded simple liquids and most polymers. These liquids show a low melt viscosity and a VFT temperature that is close to the kinetically observed glass transition.

The bulk metallic glass former studied in the present investigation shows a behavior that is similar to the relatively strong sodium silicate glass forming liquids. This strong liquid nature implies unusually high equilibrium melt viscosities of the order of 10 Pa s. These high melt viscosities were measured for the $Zr_{46.75}Ti_{8.25}Cu_{7.5}Ni_{10}Be_{27.5}$ and the $Zr_{41.2}Ti_{13.8}Cu_{12.5}Ni_{10}Be_{22.5}$ alloys [25, 26]. The data are included in Fig. 6. They are in good agreement with the low temperature data presented in this study. The bulk metallic glass forming liquids are about three orders of magnitude more viscous at the melting point than all pure metals and alloys that have been investigated thus far.

The high viscosity of bulk metallic glass forming liquids is an important contributing factor to the superior glass forming ability of these materials since it implies sluggish kinetics in the entire range of the supercooled liquid. Figure 7 compares the viscosity of the $Zr_{46.75}Ti_{8.25}Cu_{7.5}Ni_{10}Be_{27.5}$ alloy with other metallic glass forming liquids. It can be seen that alloys with high glass forming ability, i.e. low critical cooling rate, are stronger metallic glass formers than thermally less stable metallic liquids.

The high melt viscosities in multicomponent bulk metallic glass forming liquids must have structural origin. There are several experimental findings that shed some light on the structure of bulk metallic glasses:

1. Specific volume measurements of the liquid and the crystalline state by electrostatic levitation show that the density difference between liquid and solid state is relatively small for the Zr–Ti–Cu–Ni–Be alloys [30]. This means that these materials have a small free volume in the liquid at the melting point and upon supercooling.
2. In addition, it is found that the entropy of fusion in bulk metallic glass forming liquids is small [11, 21, 28]. This suggests that there is pronounced chemical short-range order present in the melt. In fact, atom probe field ion microscopy and small angle neutron scattering experiments show that this chemical short-range ordering can result in clustering [31] or phase separation [32, 33].
3. The thermal and electrical conductivity of Zr–Ti–Cu–Ni–Be bulk metallic glasses is smaller than in previously known glass forming alloys.

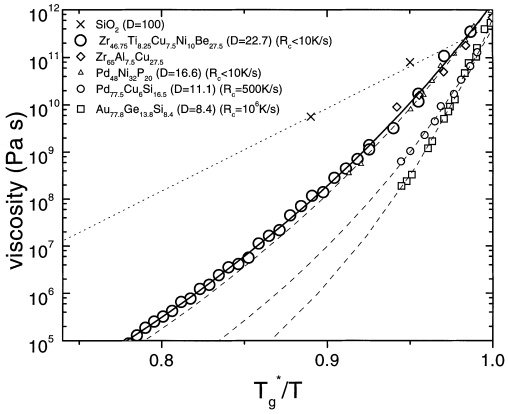

Fig. 7. Fragility plot that compares the $Zr_{46.75}Ti_{8.25}Cu_{7.5}Ni_{10}Be_{27.5}$ alloy with other bulk metallic glass forming alloys and conventional metallic glasses (◇ [29]; △, ○ [5]; □ [3]).

This suggests that an increasing number of electrons become localized in bulk metallic glasses as a result of directional bonds.

It is likely that the tendency to develop chemical short-range order, the increasing amount of directional bonds and the small amount of free volume makes the liquid more rigid with respect to shear flow and thus a strong glass former.

Chemical short-range order also implies that the supercooled liquid is thermodynamically closer to the crystalline ground state compared to conventional glass formers as was shown for several bulk glass forming alloys [34]. This reduces the thermodynamic driving force for crystallization.

4.2. Relaxation of the viscosity in the glass transition region

In the following, the relaxation of the viscosity from the amorphous state into the supercooled liquid state will be discussed. As shown in Fig. 3 the viscosity of the alloy measured at a constant heating rate is found to be smaller than the equilibrium value for temperatures below the calorimetrically observed glass transition in a DSC. The slope of the viscosity curve is shallower than for the equilibrium viscosity in the supercooled liquid. This might lead to the conclusion that there is a well-defined temperature dependence of the viscosity in the amorphous state that exhibits an activation energy different from that of the supercooled liquid state.

However, as mentioned above, the viscosity relaxes into the supercooled liquid in the same temperature interval where the calorimetric glass transition is observed using the identical heating rate. Consequently, a smaller heating rate shifts the glass transition to lower temperatures and leads to a different viscosity curve in the amorphous state. Figure 8 shows the example of two non-equilibrium viscosity measurements in the glass transition region. The sample that is heated with a smaller rate shows a larger viscosity at a certain temperature compared to the alloy that is heated with higher rate. Both samples are in a different relaxation state compared to the final equilibrium state. No well-defined equilibrium viscosity can be assigned to the frozen-in amorphous state.

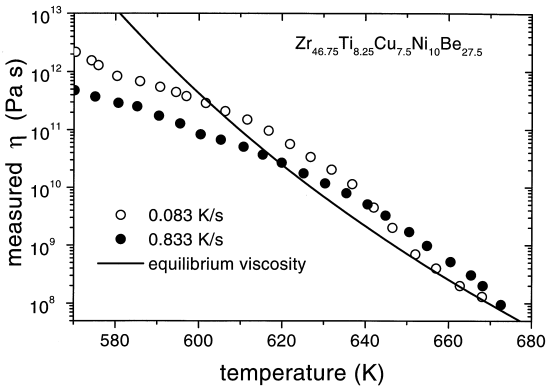

Fig. 8. Measured non-equilibrium viscosity in the glass transition region for two different heating rates.

At temperatures where the material is still amorphous using the lowest feasible heating rate, isothermal measurements are the most suitable means of obtaining an equilibrium viscosity. Viscosity under isothermal conditions relaxes to a final state that corresponds to the viscosities expected from the VFT behavior in the supercooled liquid as can be seen in Figs 3 and 5. According to the isothermal experiments there are no indications that the viscosity of this material relaxes into any well-defined amorphous metastable equilibrium state. At temperatures where the relaxation can be obtained in laboratory times ($\leq$10 days) the equilibrium state always consists of a supercooled liquid for this strong glass former. However, strictly speaking, this has to be observed on a long time scale [21].

Fitting of the viscosity relaxation with a stretched exponential function equation (4) leads to the determination of an average shear flow relaxation time τ_s and of the stretching exponent β. The stretching exponent for this type of relaxation is found to be close to 0.8 and increases slightly with temperature. This large stretching exponent is consistent with the strong liquid nature of the material. Fragile liquids, in contrast, exhibit larger deviations from exponential relaxation with stretching exponents of the order of 0.5 at the glass transition. The stretching exponent can be connected with D^*, T_0 and T_g^* as (see, e.g. Ref. [35] or Ref. [36])

$$\beta = 1 - \sqrt{\frac{(T_0/T_g^*)^2}{D}}. \tag{6}$$

Using this equation a stretching exponent of $\beta = 0.86$ can be calculated which is close to the above value obtained by fitting the viscosity relaxation.

The relaxation time in the glass transition region is proportional to the equilibrium viscosity as shown in the inset in Fig. 5. This means that both quantities in the first approximation obey the same VFT relation. The high frequency shear modulus $G_\infty = \eta/\tau$ at the glass transition is found to be 6.8×10^8 Pa.

The above considerations dealt with the relaxation kinetics of the viscosity from the amorphous state into the supercooled liquid state. In the following, the temperature dependence of the viscosity is compared with the calorimetrically observed enthalpy relaxation of the specific heat capacity as a function of heating rate.

4.3. Kinetic glass transition and viscosity

It was shown in Fig. 3 that the viscosity and the specific heat capacity relax in the same temperature interval when both quantities are measured with the

same heating rate. This holds over a range of heating rates of at least three orders of magnitude as can be seen in Fig. 4. The time scale for viscosity relaxation, τ_η^{tot}, equals the total relaxation time for the calorimetric glass transition, $\tau_{T_g}^{\mathrm{tot}}$. The total relaxation time in the glass transition range can be approximated as

$$\tau_{T_g}^{\mathrm{tot}} = \Delta T_g / R \tag{7}$$

where, ΔT_g, is the width of the glass transition region and R the heating rate. $T_g(R)$ may be defined as the center of the glass transition range or in this case as the temperature, T^*, of the steepest increase of the specific heat capacity. In Fig. 9 the equilibrium viscosity is compared with the total relaxation time as a function of $T_g(R)$. The viscosity is fitted with the VFT equation (5). The total relaxation time $\tau_{T_g}^{\mathrm{tot}}$ is fitted with the equation

$$\tau_{T_g}^{\mathrm{tot}}(T^*) = \tau_0 \cdot \exp\left(\frac{D^* \cdot T_0}{T^* - T_0}\right). \tag{8}$$

A VFT-type equation to describe the heating rate dependence of T_g was previously utilized by Brüning and Samwer [37]. The viscosity axis and the time axis in Fig. 9 are shifted, to bring the data to agreement in the glass transition region. Both fits yield very similar D^* and T_0 values. This reveals that the measured heating rate dependence of the glass transition reflects the relaxation time of the supercooled liquid as well as the temperature dependence of viscosity in the supercooled liquid.

Consequently, the heating rate dependence of the glass transition reflects the fragility of the material. A glass with a small heating rate dependence of the calorimetric glass transition is more fragile than a glass with a large heating rate dependence.

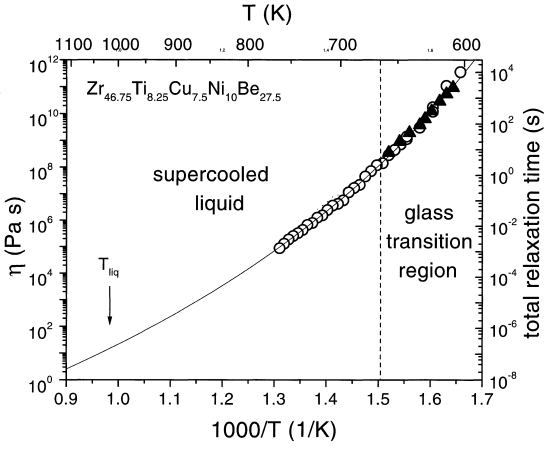

Fig. 9. Equilibrium viscosity (○) and total relaxation time (▲) at the glass transition as a function of temperature. The total relaxation time at the glass transition was calculated according to equation (7). Viscosity and total relaxation time are fitted with equations (5) and (8), respectively. Only the fit to equation (5) is shown in the plot.

4.4. Kinetic glass transition and fragility

The above considerations give a tool to estimate the fragility of a metallic glass former. Measuring the heating rate dependence of the glass transition, the change of the relaxation time close to T_g is determined. As shown above, the total relaxation time can be determined if the complete glass transition range is accessible in the experiment according to equation (7). In conventional metallic glass forming systems only the onset of the glass transition is observable in most cases. In order to compare a large number of alloys, especially with relatively poor thermal stability of the supercooled liquid, it is desirable to use the shift of the onset of T_g with heating rate to determine the fragility.

In Fig. 10, the inverse heating rate is plotted as a function of onset of glass transition normalized to T_g', which is defined as the onset of the glass transition measured at 0.0167 K/s. At this heating rate, T_g' is usually close to T_g^*, where the equilibrium viscosity is 10^{12} Pa s (see Figs 3 and 4). On the fragility plot, data are shown for different metallic glass formers. Complementary viscosity data are available for the $Zr_{46.75}Ti_{8.25}Cu_{7.5}Ni_{10}Be_{27.5}$ (this work), $Zr_{41.2}Ti_{13.8}Cu_{12.5}Ni_{10}Be_{22.5}$ [38] and the $Mg_{65}Cu_{25}Y_{10}$ [27] alloys. The fragility parameters and VFT temperatures that are determined from the viscosity data are in excellent agreement with the values obtained from fitting the relaxation a the glass transition using the shift of the onset of T_g with heating rate. Thus the heating rate dependence of the onset of T_g can be used as a measure for the

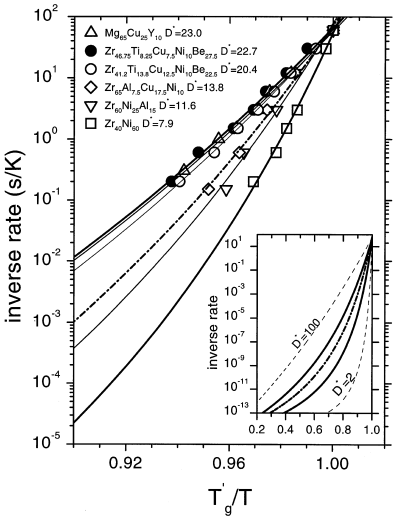

Fig. 10. Inverse heating rate as a function of onset temperature of the glass transition normalized to the onset temperature of the glass transition measured with a rate of 0.0167 K/min. The data were fitted with a VFT-type equation. The fragility parameter D^* and the VFT temperatures for the $Mg_{65}Cu_{25}Y_{10}$ alloy and both Be-bearing alloys are in excellent agreement with the values obtained after fitting the viscosity data. In the case of the other three alloys viscosity measurements do not exist.

fragility of the glass, even if the supercooled liquid is experimentally not accessible. It is not surprising that the most fragile glass in Fig. 10 is the binary $Zr_{40}Ni_{60}$ alloy. The rapid increase of the relaxation kinetics with rising temperature reduces its thermal stability with respect to crystallization.

5. SUMMARY AND CONCLUSIONS

The flow and relaxation behavior of the $Zr_{46.75}Ti_{8.25}Cu_{7.5}Ni_{10}Be_{27.5}$ bulk metallic glass forming liquid was investigated by three-point beam bending, parallel plate rheometry as well as differential scanning calorimetry. The viscosity measurements reveal that the alloy is a strong liquid similar to silicate liquids. The viscosity relaxation and enthalpy relaxation during the calorimetric glass transition reflect the kinetics in the equilibrium supercooled liquid. Complete relaxation leads to a state that is equivalent to a supercooled liquid. A metastable amorphous state could not be observed.

The strong liquid behavior implies sluggish kinetics in the supercooled liquid and at the glass transition. This is a contributing factor to the high glass forming ability of bulk metallic glass forming liquids. Less favorable metallic glass formers are more fragile. Even though the supercooled liquid of these materials is not accessible on laboratory time scales, the fragility is revealed by their low viscosities at the melting point and the small heating rate dependence of the kinetic glass transition. This small heating rate dependence reflects the faster change of the kinetics upon heating in the glass transition region compared to strong liquids.

Acknowledgements—This work was supported by the U.S. Department of Energy (Grant No. DEFG-03-86ER45242). Partial support for R. Busch was provided by the Alexander von Humboldt Foundation via the Feodor Lynen Program.

REFERENCES

1. Klement, W., Willens, R. and Duwez, P., *Nature*, 1960, **187**, 869.
2. Duwez, P., *Trans. Am. Soc. Metals*, 1967, **60**, 607.
3. Chen, H. S. and Turnbull, D., *J. chem. Phys.*, 1968, **48**, 2560.
4. Tsao, S. S. and Spaepen, F., *Acta metall.*, 1985, **33**, 1355.
5. Chen, H. S., *J. Non-Cryst. Solids*, 1978, **27**, 257.
6. Volkert, C. A. and Spaepen, F., *Acta metall.*, 1989, **37**, 1355.
7. Inoue, A., Zhang, T. and Masumoto, T., *Mater. Trans. JIM*, 1991, **31**, 425.
8. Zhang, T., Inoue, A. and Masumoto, T., *Mater. Trans. JIM*, 1991, **32**, 1005.
9. Peker, A. and Johnson, W. L., *Appl. Phys. Lett.*, 1993, **63**, 2342.
10. Kim, Y. J., Busch, R., Johnson, W. L., Rulison, A. J., Rhim, W. K. and Isheim, D., *Appl. Phys. Lett.*, 1994, **65**, 2136.
11. Busch, R., Kim, Y. J. and Johnson, W. L., *J. appl. Phys.*, 1995, **77**, 4039.
12. Geyer, U., Schneider, S., Johnson, W. L., Qiu, Y., Tombrello, T. A. and Macht, M. P., *Phys. Rev. Lett.*, 1995, **75**, 2364.
13. Busch, R., Kim, Y. J., Johnson, W. L., Rulison, A. J. and Rhim, W. K., *Appl. Phys. Lett.*, 1995, **66**, 3111.
14. Stephan, M. J., *Akad. Wiss. Wien. Math.-Natur Klasse Abt. 2*, 1884, **69**, 713.
15. Diennes, G. J. and Klemm, H. F., *J. appl. Phys.*, 1946, **17**, 458.
16. Bakke, E., Busch, R. and Johnson, W. L., *Appl. Phys. Lett.*, 1995, **67**, 3260.
17. Bakke, E., Busch, R. and Johnson, W. L., *Mater. Sci. Forum*, 1996, **225-227**, 95.
18. Hagy, H. E., *J. Am. Ceram. Soc.*, 1963, **46**, 93.
19. Trouton, F. T., *Proc. R. Soc. Lond.*, 1906, **77**, 426.
20. Reiner, M., in *Rheology*, Vol. 1, ed. F. R. Eirich. Academic Press, New York, 1956, p. 9.
21. Busch, R. and Johnson, W. L., *Appl. Phys. Lett.*, 1998, **72**, 2695.
22. Phillips, J. C., *Rep. Prog. Phys.*, 1996, **59**, 1133.
23. Angell, C. A., *Science*, 1995, **267**, 1924.
24. Nemilov, S. V., *Glass Physics Chemistry*, 1995, **21**, 91.
25. Masuhr, A., Ph.D. thesis, California Institute of Technology, 1998.
26. Busch, R., Masuhr, A., Bakke, E. and Johnson, W. L., *Mater. Res. Soc. Symp. Proc.*, 1997, 455.
27. Adam, G. and Gibbs, J. H., *J. chem. Phys.*, 1965, **43**, 139.
28. Busch, R., Liu, W. and Johnson, W. L., *J. appl. Phys.*, 1998, **83**, 4134.
29. Rambousky, R., Moske, M. and Samwer, K., *Z. Phys.*, 1996, **B99**, 387.
30. Ohsaka, K., Chung, S. K., Rhim, W. K., Peker, A., Scruggs, D. and Johnson, W. L., *Appl. Phys. Lett.*, 1997, **70**, 726.
31. Miller, M. K., Russell, K. F., Martin, P. M., Busch, R. and Johnson, W. L., *J. Physique IV*, 1996, **6**(C5), 217.
32. Busch, R., Schneider, S., Peker, A. and Johnson, W. L., *Appl. Phys. Lett.*, 1995, **67**, 1544.
33. Schneider, S., Thiyagarajan, P. and Johnson, W. L., *Appl. Phys. Lett.*, 1996, **68**, 493.
34. Busch, R., Bakke, E. and Johnson, W. L., *Mater. Sci. Forum*, 1997, **235-238**, 327.
35. Vilgis, T. A., *Phys. Rev.*, 1993, **B47**, 2882.
36. Böhmer, R., Ngai, K. L., Angell, C. A. and Plazek, D. J., *J. chem. Phys.*, 1993, **99**, 4201.
37. Brüning, R. and Samwer, K., *Phys. Rev. B,* 1992, **46,** 11318.
38. Waniuk, A., Busch, R. and Johnson, W. L., *Acta mater.* (submitted).